Study on novel physiological function of 1-deoxynojirimycin derived from mulberry leaves

著者	Shung E
学位授与機関	Tohoku University
学位授与番号	11301甲第18742号
URL	http://hdl.handle.net/10097/00125728

Study on novel physiological function of 1-deoxynojirimycin derived from mulberry leaves

（桑葉由来 1-デオキシノジリマイシンの新規生理機能に

関する研究）

Shuang E

Table of contents

Chapter 1: 1-Deoxynojirimycin attenuates high glucose-accelerated senescence in human umbilical vein endothelial cells

Chapter 2: Intake of mulberry 1-deoxynojirimycin prevents colorectal cancer in mice

1-Deoxynojirimycin attenuates high glucose-accelerated senescence in human umbilical vein endothelial cells

1. Abstract

The influence of 1-deoxynojirimycin (DNJ) derived from mulberry on senescence of endothelial cells was examined with the goal of discovery of a method for prevention of senescence of blood vessels. The effect of DNJ on senescence of human umbilical vein endothelial cells (HUVECs) promoted under high glucose condition was determined. HUVECs were cultured in normal glucose (5.6 mmol/L, NG group), normal glucose plus DNJ (10 μmol/L, DNJ group), high glucose (30 mmol/L, HG group), or high glucose plus DNJ (10 μmol/L, HG + DNJ group) and passaged until they reached senescence. The proliferation rate was markedly decreased in the HG group compared with the NG group, and this phenomenon was reversed by DNJ. The frequency of senescent (SA-ß-Gal-positive) cells and the expression level of senescence genes (PAI-1 and p21) were significantly higher in the HG group compared with the NG group, and these changes were blocked by DNJ. Monocyte adhesion, NF-kB activity, and reactive oxygen species production, all of which promote cellular senescence, were significantly increased in the HG group compared with the NG

group, and again these changes were blocked by DNJ. Therefore, these results show that DNJ delays cellular senescence that is promoted under high glucose condition.

2. Abbreviations

DNJ: 1-Deoxynojirimycin

HUVEC: human umbilical vein endothelial cells

ROS: reactive oxygen species

HILIC-QTRAP MS/MS: hydrophilic interaction liquid chromatography with hybrid quadrupole/linear ion trap tandem mass spectrometry

hEGF: human epidermal growth factor

hFGF-B: human basic fibroblast growth factor

PDL: Population doubling level

CPDL: cumulative population doubling level

ICAM1: intercellular adhesion molecule 1

SELE: selectin E

VCAM1: vascular cell adhesion molecule 1

H2DCFDA: 2′,7′-Dichlorodihydrofluorescein diacetate

3. Introduction

Lifestyle-related diseases such as diabetes mellitus and arteriosclerosis are increasing yearly and can progress to cerebral and cardiac diseases [10, 11]. Elderly persons are mainly affected and these conditions are referred to as aging-related diseases. Thus, prophylaxis for these diseases is important for maintenance of a healthy life. Aging progresses gradually and a method of delaying of senescence through food intake may be effective for prevention of aging-related disease. Senescent vascular endothelial cells have been found in arteriosclerotic sites in humans, which indicates a possible relationship of these cells with an aging-related disease [12]. We recently found that senescence of vascular endothelial cells is promoted by monocyte adhesion [30]. Senescence of blood vessels is also promoted by reactive oxygen species (ROS), the production of which increases when the blood glucose level is high, such as in patients with diabetic mellitus [6, 17, 30, 31]. Therefore, suppression of intracellular ROS production is likely to be effective for senescence delay.

1-Deoxynojirimycin (DNJ) may be a food constituent that delays senescence of blood vessels. DNJ is derived from mulberry (Moraceae) and has a chemical structure like that of glucose (Figure 1) [29]. DNJ inhibits α-glucosidase in the small bowel mucosa, which reduces absorption of sugar and suppresses after-meal hyperglycemia [1, 8, 14, 28]. We have also shown that DNJ reduces oxidative stress in the liver and

plasma in rodents [8, 28]. Therefore, DNJ may also delay senescence of endothelial cells induced by oxidative stress, but this effect of DNJ is not clear. In this study, we examined whether DNJ can delay senescence of endothelial cells promoted under high glucose condition, with the goal of discovering a method for prevention of aging-related diseases.

Senescent cells were prepared by culturing human umbilical vein endothelial cells (HUVECs) until they reached the Hayflick limit [30]. Senescence of HUVECs is promoted under high glucose condition, and thus a culture in high glucose was used (19, 31, 32). Since the plasma DNJ level reaches 3.2 μmol/L in human receiving a small amount of DNJ (6.3 mg) [16] and 100 μmol/L in rat receiving DNJ (110 mg/kg of body weight) [15], it was thought that DNJ can reach 10 μmol/L in human plasma. Therefore, DNJ in the culture medium was adjusted to 10 μmol/L. HUVECs were cultured in normal glucose (NG), normal glucose plus DNJ (DNJ), high glucose (HG), or high glucose plus DNJ (HG + DNJ), and changes in cellular proliferative potential, proportion of senescent cells, and expression of senescence genes were evaluated. HUVECs also have increased expression of proteins that promote monocyte adhesion [30], which occurs in the first stage of arteriosclerosis and is promoted by NF- kB and ROS [17, 18, 21]. Thus, the effects of DNJ on monocyte adhesion and on NF-kB activity and ROS production were examined.

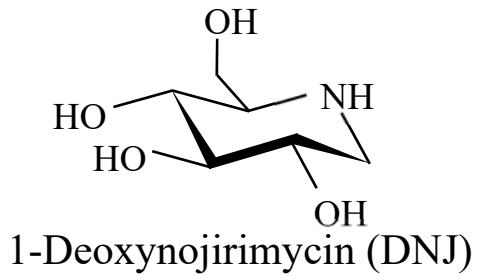

1-Deoxynojirimycin (DNJ)

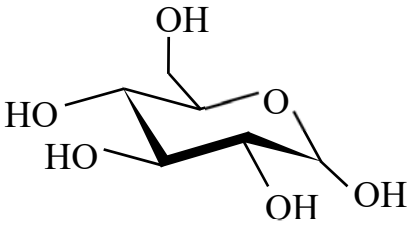

D-glucose

Figure 1. Chemical structures of 1-deoxynojirimycin (DNJ) and D-glucose.

4. Materials and methods

4.1. Materials

DNJ was extracted from mulberry leaves (Morus alba) and purified using ion-exchange chromatography followed by recrystallization [8, 15, 16]. The purity of DNJ was shown to be N98% by hydrophilic interaction liquid chromatography with hybrid quadrupole/linear ion trap tandem mass spectrometry (HILIC-QTRAP MS/MS) [16].

4.2. Cells and cell culture

HUVECs were purchased from Kurabo (Osaka, Japan) and cultured in HuMedia-EG2 growth medium (Kurabo, Osaka, Japan) at 37 °C in a humidified atmosphere of 5% CO2 in air [25, 30]. HuMedia-EG2 medium consists of base medium (HuMedia-EB2) supplemented with 2% FBS, 0.5 mg/L human epidermal growth factor (hEGF), 2 mg/L human basic fibroblast growth factor (hFGF-B), 5 g/L insulin, 50 g/L gentamicin, and 50 mg/L amphotericin B. HUVEC monolayers of passage 9 were used in the experiments. THP-1 monocytes were obtained from the Cell Resource Center for Biomedical Research at Tohoku University School of Medicine (Sendai, Japan) and maintained in RPMI-1640 medium supplemented with 10% FBS, 100 units/mL penicillin, and 100

μg/mL streptomycin at 37 °C in a humidified atmosphere of 5% CO2.

4.3. Cytotoxicity of DNJ

Cytotoxicity of DNJ was assessed using a WST-8 assay [20, 24, 30]. HUVECs at 80% confluency were trypsinized and transferred to 96-well plates (4000 cells/well). Stock solutions of DNJ were prepared in HuMedia- EG2 medium. DNJ test media were prepared from the stock solutions and diluted to final concentrations of 0–200 μmol/L in HuMedia-EG2 medium. After incubation for 24 h at 37 °C, the cells were placed in 200 μL of fresh HuMedia-EG2 medium with various concentrations of DNJ. After 24 or 48 h, 10 μL WST-8 solution (Dojindo, Kumamoto, Japan) was added to each well. After incubation for 3 h at 37 °C, cytotoxicity was measured using a microplate reader (Infinit F200; Tecan Japan, Kawasaki, Japan) at a wavelength of 450 nm and a reference wavelength of 655 nm.

4.4. Preparation of senescent cells

Senescent cells were prepared by further culturing of HUVECs [30] using a culture condition in high glucose [19, 31, 32]. HUVECs were subcultured upon reaching 80% confluence using 0.25% trypsin-EDTA (Lonza, Walkersville, MD). The cells were propagated until senescence and cell numbers

were determined when subcultured by passing a 1/50 dilution of cells through a Coulter Counter [2, 30]. Population doubling level (PDL) was estimated at each passage using the following equation: n = (log2X − log2Y) (with n = PD, X = number of cells at the end of one passage, Y = number of cells that were seeded at the beginning of one passage) [19]. For each passaging, the resulting PDL estimation was added to the sum of PDL from the previous passages to achieve the cumulative population doubling level (CPDL), which was plotted against time to obtain a growth curve [19]. Since the plasma DNJ level reaches 3.2 μmol/L in human receiving a small amount of DNJ (6.3 mg) [16] and 100 μmol/L in rat receiving DNJ (110 mg/kg of body weight) [15], it was thought that DNJ can reach 10 μmol/L in human plasma. Therefore, DNJ in the culture medium was adjusted to 10 μmol/L. HUVECs were cultured in normal glucose (5.6 mmol/L, NG), normal glucose plus DNJ (10 μmol/L, DNJ), high glucose (30 mmol/L, HG), or high glucose plus DNJ (10 μmol/L, HG + DNJ) at 37 °C in a 5% CO2 atmosphere and passaged until they reached the Hayflick limit, based on no observation of cell division for 30 days [30]. Since HUVECs at PDL 28.2 reached the Hayflick limit in the HG group, in all experiments, four groups of cells were used: HUVECs at PDL28-29 exposed to NG (NG group), HUVECs at PDL28-29 exposed to NG and 10 μmol/L DNJ (DNJ group), HUVECs at PDL28-29 exposed to HG (HG group); and HUVECs at PDL28-29 exposed to HG and

10 μmol/L DNJ (HG + DNJ group).

4.5. Senescence-associated ß-galactosidase (SA-ß-gal) staining

HUVECs of the NG, DNJ, HG, and HG + DNJ groups at 80% confluency were trypsinized, transferred to 6-well plates (8000 cells/well), and preincubated in HuMedia-EG2 medium for 24 h. The cells were detected with a senescence detection kit (BioVision Inc., Mountain View, CA, USA) [3, 30]. After SA-ß-Gal staining, cells were washed once with PBS (-), 1.5 mL of Hoechst 33342 (Dojindo) (1 μg/mL) was added to each well, and the cells were incubated at room temperature for 30 min. Alteration of cellular morphology was observed by fluorescent microscopy (Biozero, Keyence, Osaka, Japan). The data were shown by the ratio to young cells (normal-glucose exposed HUVECs at PDL8-9) to indicate a change with age.

4.6. mRNA expression analysis

A quantitative reverse transcriptase-PCR assay was conducted on total RNA extracted from the liver using an RNeasy mini kit (Qiagen, Valencia, CA, USA) [25, 27, 30]. Expression levels of PAI-1, p21, intercellular adhesion molecule 1 (ICAM1), selectin E (SELE) and vascular cell adhesion molecule 1 (VCAM1) mRNA in HUVECs were determined with a Thermal Cycler Dice Real Time System

(Takara Bio, Shiga, Japan), which allowed real-time quantitative detection of the PCR products by measuring the increase in fluorescence caused by binding of SYBR green to double-stranded DNA. In brief, cDNA was made from the total RNA in HUVECs of the NG, DNJ, HG, and HG + DNJ groups using a PrimeScript RT Master Mix (Perfect Real Time) kit (Takara), and subjected to PCR amplification with SYBR Premix Ex Taq (Takara) and a gene-specific primer for ICAM1, PAI-1, p21, SELE, VCAM1 or ß-actin (Table 1). Amplification was performed with an activation step at 95 °C for 10 s, followed by 40 cycles at 95 °C for 5 s (denaturation) and 60 °C for 31 s (extension), and a dissociation stage at 95 °C for 15 s, 60 °C for 30 s and 95 °C for 15 s. The ß-actin content in each sample was used to normalize the results. The data were shown by the ratio to young cells (normal-glucose exposed HUVECs at PDL8-9) to indicate a change with age.

4.7. Monocyte adhesion assay

Monocyte adhesion assays were carried out essentially as previously described [7, 9, 30]. HUVECs of the NG, DNJ, HG, and HG + DNJ groups at 1 × 104 cells/mL were seeded in 96-well plates in complete medium (200 μL/well) and incubated at 37 °C in a 5% CO2 atmosphere for 6 h. After incubation, the cells were washed twice with RPMI-1640 medium and the medium was added to each well (100 μL/well). Calcein AM (Dojindo)-labeled THP-1 cells in RPMI-1640 medium at 2 ×

105 cells/mL were added to each well (100 μL/well) containing HUVECs and incubated at 37 °C in 5% CO2 for 10 min. After incubation, the wells were filled with RPMI-1640 medium, sealed, inverted, and centrifuged at low speed (1300 rpm) for 5 min. After nonadherent THP-1 cells were removed, 100 μL of Hoechst 33342 (1 μg/mL) was added to each well and the cells were incubated at room temperature for 30 min [26]. The numbers of HUVECs and adherent THP-1 cells were counted. The data were shown by the ratio to young cells (normal-glucose exposed HUVECs at PDL8-9) to indicate a change with age.

4.8. NF-kB activity assay

NF-kB activity was assessed using a Trans-AM NF-κB p65 transcription factor assay kit (Active Motif, Carlsbad, CA, USA) [33]. Nuclear extracts in HUVECs of the NG, DNJ, HG, and HG + DNJ groups were prepared by nuclear lysis after cell lysis. Cells were suspended in 30 μl of buffer containing 10 mM HEPES (pH 7.9), 1.5 mM MgCl2, 10 mM KCl, 0.5 mM dithiothreitol, and 0.2 mM phenylmethylsulfonyl fluoride. The cells were subjected to vigorous vortex for 15 s, allowed to stand at 4 °C for 10 min, and centrifuged at 2000 rpm for 2 min. Pelleted nuclei were resuspended in a buffer containing 20 mM HEPES (pH 7.9), 25% glycerol, 420 mM NaCl, 1.5 mM MgCl2, 0.2 mM EDTA, 0.5 mM dithiothreitol and 0.2 mM phenylmethylsulfonyl fluoride for 20 min on ice,

and then the lysates were centrifuged at 15,000 rpm for 2 min. Supernatants containing solubilized nuclear proteins were used for the NF-kB activity assay. The data were shown by the ratio to young cells (normal-glucose exposed HUVECs at PDL8-9) to indicate a change with age.

4.9. Reactive oxygen species (ROS) detection

2′,7′-Dichlorodihydrofluorescein diacetate (H2DCFDA, Wako) is a specific molecular probe for H_2O_2 [4, 5, 13, 30]. H2DCFDA diffuses through cell membranes and is enzymatically hydrolyzed by intracellular esterases to non-fluorescent dichlorofluorescein, which reacts with H2O2 to form a fluorescent compound. HUVECs of the NG, DNJ, HG, and HG + DNJ groups at 4 × 104 cells/mL were seeded in 24-well plates and preincubated in HuMedia-EG2 medium for 6 h. After incubation, cells were washed once with PBS (-) and fixed with 10% formaldehyde for 15 min at room temperature. Cells were washed once with PBS (-), 250 μL of Hoechst 33342 (1 μg/mL) was added to each well, and the cells were incubated at room temperature for 30 min [26]. Cells were washed once with PBS (-), and then 250 μL of H2DCFDA (10 μM) was added to each well and incubated at 37 °C in a 5% CO2 atmosphere for 30 min. After incubation, the fluorescence intensity at 485 nm excitation and 535 nm emission was measured using an Infinite 200 spectrometers. The data were shown by the ratio to young cells (normal-glucose exposed HUVECs at PDL8-9) to indicate

a change with age.

4.10. Statistical analysis

Results are expressed as means ± SD. To test the significance of the effects of glucose and DNJ concentrations, and their interaction, two-way ANOVA was used. When a significant interaction ($P < 0.05$) was found, individual comparisons were made by a Tukey honestly significant difference test. Significant difference was expressed as follows: $^{*}P < 0.05$, $^{**}P < 0.01$ (vs. NG); $^{\#}P < 0.05$, $^{\#\#}P < 0.01$ (vs. HG).

Table 1. Primer pairs used for qRT-PCR

Genbank ID	Gene name	Primer	Primer sequence (5’ to 3’)
NM_000201	*ICAM1*	Forward	TCTGTGTCCCCCTCAAAAGTC
		Reverse	GGGGTCTCTATGCCCAACAA
NM_000602	*PAI-1*	Forward	TGCTGGTGAATGCCCTCTACT
		Reverse	CGGTCATTCCCAGGTTCTCTA
NM_000389	*p21*	Forward	GTCACTGTCTTGTACCCTTGTG
		Reverse	CGGCGTTTGGAGTGGTAGAAA
NM_000450	*SELE*	Forward	GATGAGAGGTGCAGCAAGAAG
		Reverse	CTCACACTTGAGTCCACTGAAG
NM_011693	*VCAM1*	Forward	TGCACAGTCCCTAATGTGTATCC
		Reverse	GACTTTATGCCCATTTCCTCCA
NM_001101	*β-actin*	Forward	TGGCACCCAGCACAATGAA
		Reverse	CTAAGTCATAGTCCGCCTAGAAGCA

5. Results

5.1. Cytotoxicity of DNJ

To examine the cytotoxicity of DNJ, the survival of HUVECs at PDL8-9 exposed to DNJ (0-200 μmol/L) was examined (Figure 2). The survival rate of HUVECs exposed to 0 μmol/L DNJ for 24 or 48 h was defined as 100%. DNJ did not influence the survival of HUVECs.

5.2. Effects of high glucose and DNJ on cell proliferation

To examine the effects of high glucose and DNJ on cell proliferation in HUVECs, HUVECs exposed to high glucose and DNJ were cultured until they reached the Hayflick limit. HUVECs increased logarithmically up to PDL10 and then cell proliferation decreased with increasing PDL (Figure 3I). A particularly marked decrease in cell proliferation was observed in HUVECs exposed to high glucose compared with those exposed to normal glucose, and this change was reversed by DNJ. HUVECs in the NG, DNJ, HG, and HG + DNJ groups reached the Hayflick limit at PDL 32.7, 33.7, 28.2 and 32.0, respectively. The number of days required for HUVECs to reach PDL28 was compared (Figure 3II). Cell proliferation was significantly decreased in the HG group compared with the NG group and this decrease was blocked by DNJ. There was no significant difference

between NG and DNJ groups.

5.3. Effects of high glucose and DNJ on cellular senescence

HUVECs were evaluated by a SA-ß-Gal staining assay to detect senescent cells and observe the progression of senescence with increasing PDL. HUVECs at PDL28-29 in the NG group were larger than the cells at PDL8-9, and the rates of SA-ß-Gal-positive cells at PDL28-29 were significantly higher than at PDL8-9 (data not shown). The rate of SA-ß-Gal-positive cells was significantly higher in the HG group compared with the NG group and this increase was suppressed by DNJ (Figure 4). Additionally, the rate of SA-ß-Gal-positive cells was significantly lower in the DNJ group compared with the NG group. mRNA levels for PAI-1 and p21, which are upregulated by aging in HUVECs, were also significantly higher in HUVECs at PDL28-29 than at PDL8-9 in a quantitative RT-PCR assay (data not shown). The mRNA levels of PAI-1 and p21 were also significantly higher in the HG group compared with the NG group and this increase was also suppressed by DNJ (Table 2). Additionally, the mRNA level of PAI-1 was also significantly lower in the DNJ group compared with the NG group.

5.4. Effects of high glucose and DNJ on monocyte adhesion

To examine the effects of high glucose and DNJ on monocytic adhesion, HUVECs and calcein AM-labeled THP-1 cells were co-cultured. Monocytic adhesion with HUVECs at PDL28-19 in the NG group was significantly higher than that with cells at PDL8-9 (data not shown). Monocytic adhesion was significantly greater in the HG group compared with the NG group and this increase was suppressed by DNJ (Figure 5). There was no significant difference between NG and DNJ groups. mRNA levels of ICAM1, SELE, and VCAM1, which are cell adhesion molecules, were significantly higher in HUVECs at PDL30 than at PDL9 in a quantitative RT-PCR assay (data not shown). These mRNA levels were also significantly higher in the HG group compared with the NG group and these increases were suppressed by DNJ (Table 2). Additionally, the mRNA levels of ICAM1 and VCAM1 were significantly lower in the DNJ group compared with the NG group.

5.5. Effects of high glucose and DNJ on NF-kB activity and ROS generation

Monocyte adhesion in HUVECs is promoted by NF-kB activation and ROS generation. NF-kB activity in HUVECs at PDL28-29 was significantly higher than that at PDL8-9 (data not shown) and was significantly higher in the HG group compared with the NG group, with this increase was suppressed by DNJ (Figure 6I). Additionally, NF-kB activity was significantly lower in the DNJ

group compared with the NG group. An H2DCFDA assay showed that ROS generation in HUVECs at PDL28-29 was also significantly higher than that at PDL8-9 (data not shown). ROS generation was also significantly higher in the HG group compared with the NG group and this increase was suppressed by DNJ (Figure 6II). Additionally, ROS generation was also significantly lower in the DNJ group compared with the NG group.

Table 2. Effects of DNJ on mRNA expression for genes related to cellular senescence and monocyte adhesion.

Gene name	NG	DNJ	HG	HG+DNJ
PAI-1	3.63 ± 0.37	2.53 ± 0.37*	5.45 ± 0.59*	2.68 ± 0.47$^{\#\#}$
p21	2.12 ± 0.18	2.09 ± 0.09	4.41 ± 0.34**	2.87 ± 0.37$^{\#}$
ICAM1	6.44 ± 1.06	3.44 ± 0.66*	16.14 ± 2.30**	4.01 ± 0.25$^{\#\#}$
SELE	7.73 ± 1.93	6.99 ± 0.83	23.00 ± 3.63**	9.52 ± 1.73$^{\#\#}$
VCAM1	6.64 ± 0.89	5.04 ± 0.51*	13.66 ± 2.30*	5.49 ± 2.12$^{\#}$

The mRNA expression of 5 genes related to cellular senescence and adhesion molecules in NG, DNJ, HG, and HG+DNJ groups was determined by using qRT-PCR. The data were shown by the ratio to young cells (normal-glucose exposed HUVECs at PDL8-9). Values are expressed as the mean ± SD (n=10). $^{*}P < 0.01$, $^{**}P < 0.01$ (vs. NG); $^{\#}P < 0.05$, $^{\#\#}P < 0.01$ (vs. HG). NG; normal-glucose exposed HUVECs at PDL28-29, DNJ; normal-glucose and 10 μmol/L DNJ exposed HUVECs at PDL28-29, HG; high-glucose exposed HUVECs at PDL28-29, HG+DNJ; high-glucose and 10 μmol/L DNJ exposed HUVECs at PDL28-29.

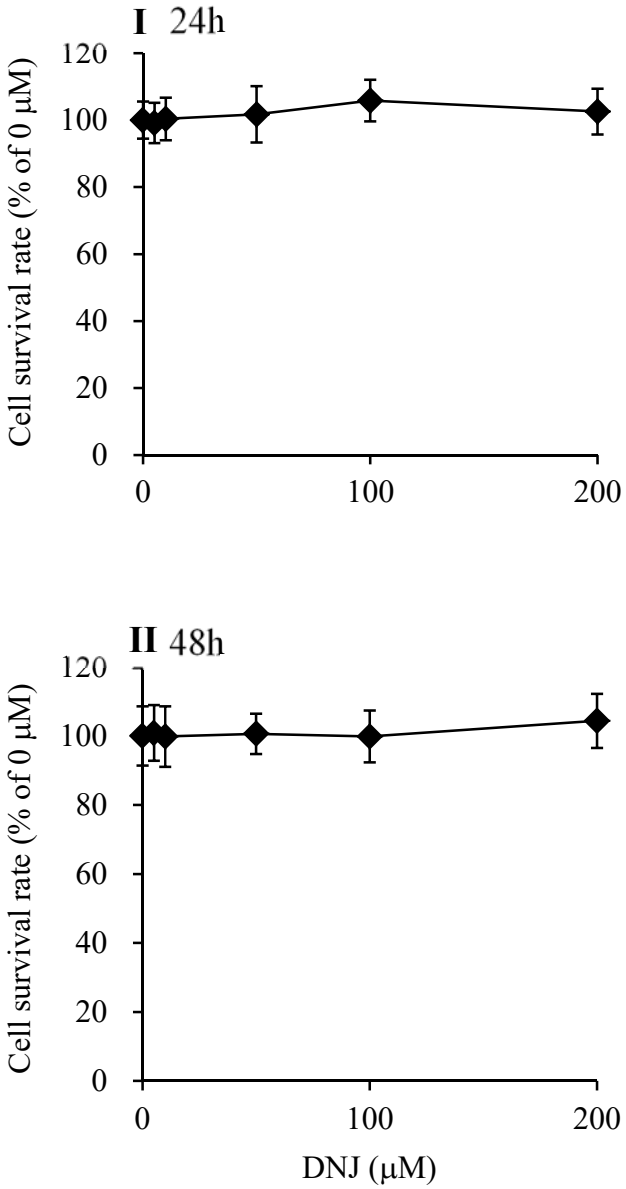

Figure 2. Cytotoxicity of DNJ in HUVECs at PDL8-9. Cell survival rates of HUVECs exposed to DNJ for 24 h (I) and 48 h (II) were examined by WST-8 assay. Values are expressed as the mean ± SD (n = 6).

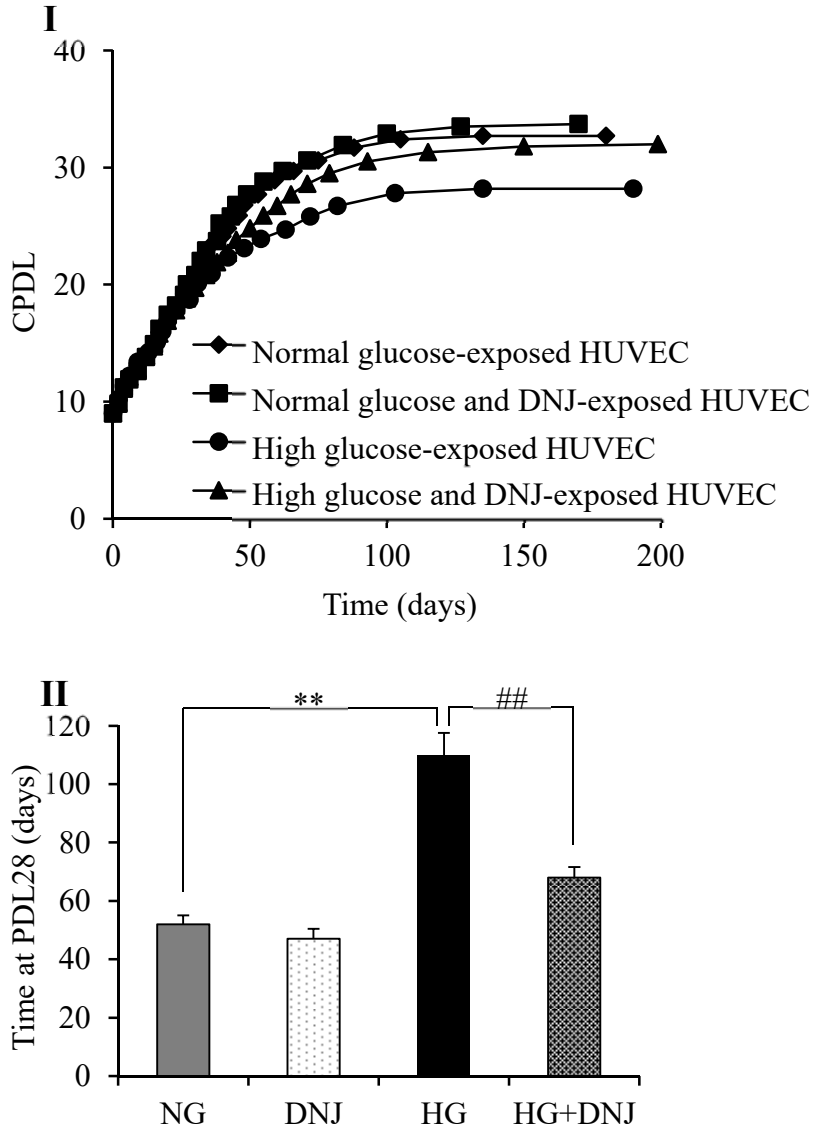

Figure 3. Effects of DNJ on cell proliferation in HUVECs exposed to high glucose. (I) Growth curve showing the cumulative population doubling level (CPDL) during culturing from young to senescent. HUVECs exposed to normal glucose (NG), NG + DNJ (10 μmol/L), high glucose (HG), and HG + DNJ (10 μmol/L) were cultured until they became senescent. (II) The number of days required for HUVEC to reach PDL28 was compared. Values are expressed as the mean ± SD (n = 10). *P < 0.05, **P < 0.01 (vs. NG). #P b 0.05, ##P b 0.01 (vs. HG).

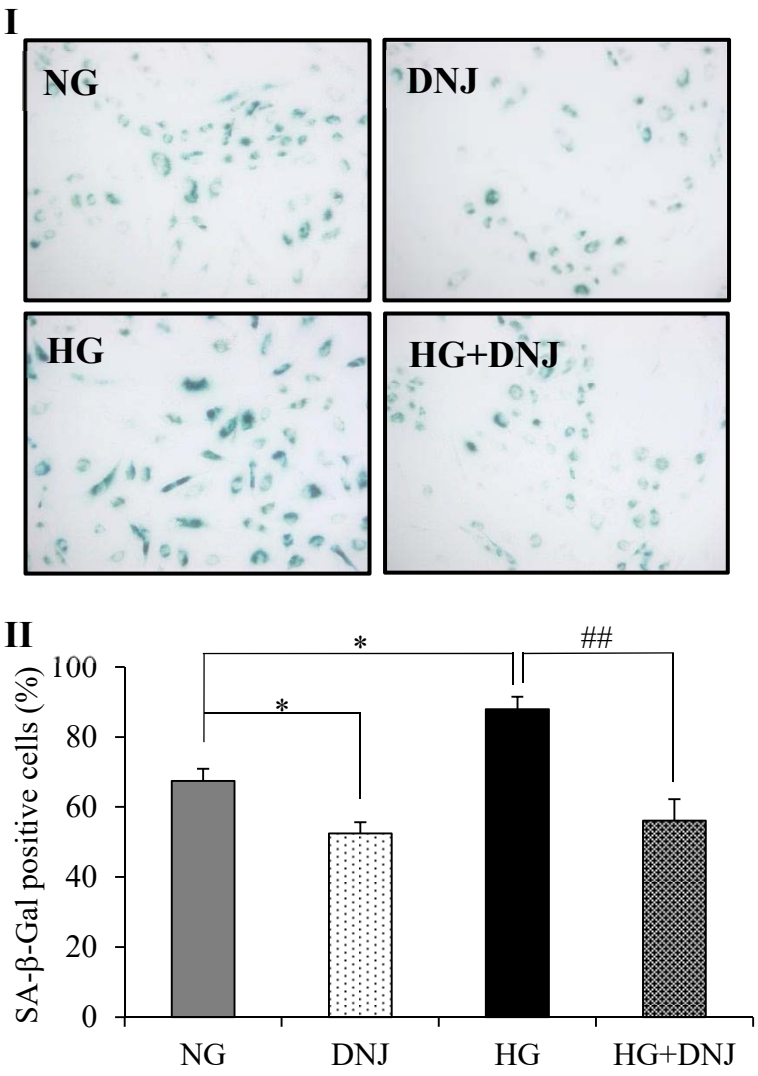

Figure 4. Effects of DNJ on senescence of HUVECs exposed to high glucose. (I) Photographs of typical SA-ß-Gal-stained HUVECs in the NG, DNJ, HG, and HG + DNJ groups. (II) Percentages of SA-ß-Gal-positive HUVECs in the NG, DNJ, HG, and HG + DNJ groups. The data were shown by the ratio to young cells (normal-glucose exposed HUVECs at PDL8-9). Values are expressed as the mean ± SD (n = 10). *P < 0.05, **P < 0.01 (vs. NG). #P < 0.05, ##P < 0.01 (vs. HG).

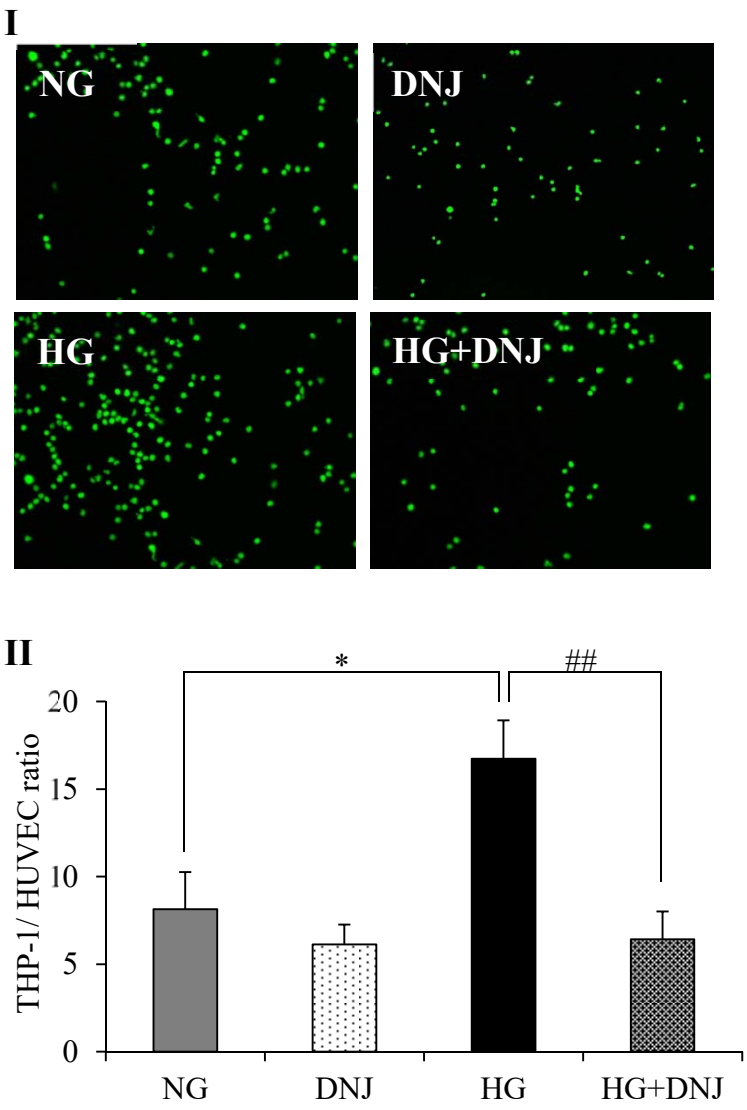

Figure 5. Effects of DNJ on monocyte adhesion. (I) Photographs of typical fluorescence- stained THP-1 cells in HUVECs in the NG, DNJ, HG, and HG + DNJ groups. (II) Percentages of THP-1 cells in HUVECs in the NG, DNJ, HG, and HG + DNJ groups. The data were shown by the ratio to young cells (normal-glucose exposed HUVECs at PDL8-9). Values are expressed as the mean ± SD (n = 10). *P < 0.05, **P < 0.01 (vs. NG). #P < 0.05, ##P < 0.01 (vs. HG).

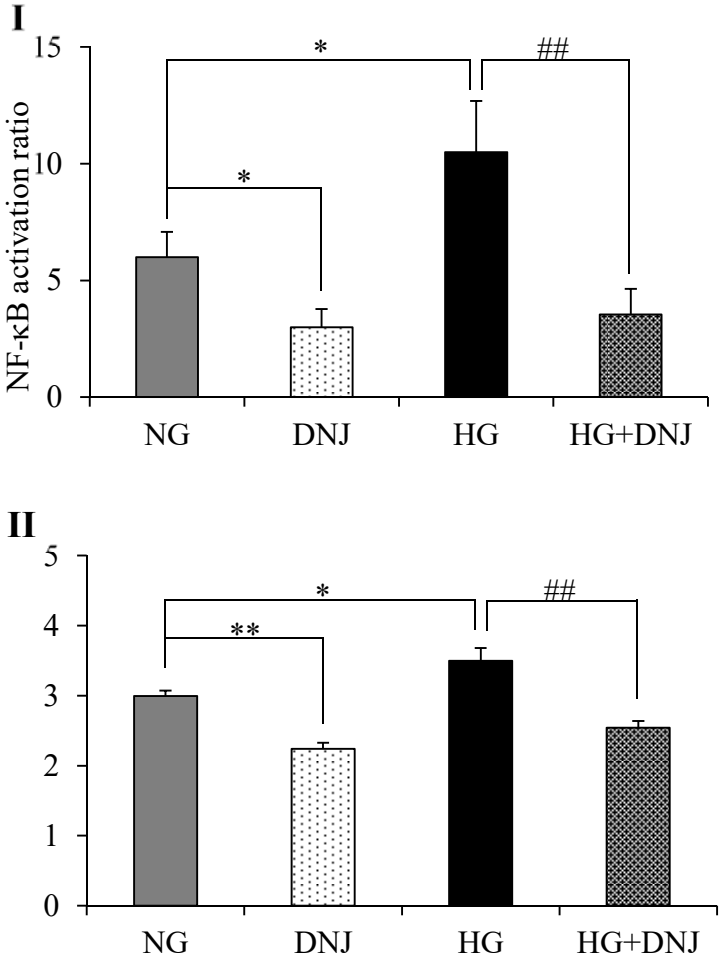

Figure 6. Effects of DNJ on NF-kB activation and ROS generation in high-glucose exposed HUVECs. (I) Proportion of NF-kB activation in the NG, DNJ, HG, and HG + DNJ groups. (II) ROS generation in the NG, DNJ, HG, and HG + DNJ groups based on a H2DCFDA assay. The data were shown by the ratio to young cells (normal-glucose exposed HUVECs at PDL8-9). Values are expressed as the mean ± SD (n = 10). *P < 0.05, **P < 0.01 (vs. NG). #P < 0.05, ##P < 0.01 (vs. HG).

6. Discussion

Delayed senescence of endothelial cells promoted by DNJ may be effective for prevention of aging-related diseases. In this study, we showed for the first time that DNJ can delay senescence of HUVECs that is promoted under high glucose condition. Since there has been no report of the cytotoxicity of DNJ in HUVECs, we first showed that DNJ up to 200 μmol/L did not influence survival of HUVECs. We have also shown previously that the DNJ level in human plasma can reach 3.2 μmol/L [16] and in rat plasma about 100 μmol/L [15], and therefore a level of 10 μmol/L was used to evaluate the effects of DNJ on the senescence of endothelial cells.

A marked decrease in cell proliferation was observed in HUVECs exposed to high glucose compared to those cultured with normal glucose. SA-ß-Gal-positive cells in these groups were significantly more frequent than in young cells, and significantly more frequent in the HG group compared with the NG group. mRNA levels of PAI-1 and p21, which are upregulated by senescence in HUVECs, were significantly higher in the NG group compared to young cells, and significantly higher in the HG group compared with the NG group. The decrease in cell proliferation and increases in SA-ß-Gal-positive cells and mRNA levels of PAI-1 and p21 were reversed by DNJ. These findings suggest that DNJ attenuates high glucose-accelerated senescence in HUVECs and

may be effective for prevention of aging-related diseases. Additionally, the rate of SA-ß- Gal-positive cells and the mRNA level of PAI-1 were significantly lower in the DNJ group compared with the NG group. Therefore, DNJ might be effective also for delay senescence.

We have previously shown that senescence HUVECs have increased levels of genes related to monocyte adhesion [30]. In this study, senescence of HUVECs promoted monocyte adhesion and this effect was markedly increased by high glucose and suppressed by DNJ. Monocyte adhesion occurs in the first stage of arteriosclerotic [21]. Therefore, intake of DNJ might be effective for prophylaxis of arteriosclerosis. Expression of monocyte adhesion molecules is induced by NF-kB and ROS [17, 18], and we found that senescence of HUVECs increased ROS production which activated NF-kB, with these changes promoted by high glucose and suppressed by DNJ. We previously showed that DNJ reduced oxidative stress in the liver and plasma of mice and rats [22, 23]. Additionally, in this study, ROS generation was significantly lower in the DNJ group compared with the NG group. These findings suggest that DNJ behaves as an antioxidant, decreases ROS production, and delays cellular senescence. Attenuation of high glucose-accelerated senescence by decreasing ROS levels may make DNJ useful as a health food supplement and medicine. Further studies are needed to determine the mechanisms underlying these effects. Additionally, we previously reported that DNJ

is quickly eliminated from the body [15, 16]. Hence, in the case of considering the application to humans, it is necessary to ingest many times, to obtain the effect of DNJ. For example, it may be necessary to drink the mulberry tea (DNJ-rich food) several times at meal [34].

7. References

(1) Asano, N., Nash, R.J., Molyneux, R.J., Fleet, G.W.J., 2000. Sugar-mimic glycosidase inhibitors: natural occurrence, biological activity and prospects for therapeutic application. *Tetrahedron-Asymmetry* 11, 1645–1680.

(2) Boisen, L., Drasbek, K.R., Pedersen, A.S., Kristensen, P., 2010. Evaluation of endothelial cell culture as a model system of vascular ageing. *Exp. Gerontol.* 45, 779–787.

(3) Dimri, G.P., Lee, X., Basile, G., Acosta, M., Scott, G., Roskelley, C., Medrano, E.E., Linskens, M., Rubelj, I., Pereira-Smith, O., 1995. A biomarker that identifies senescent human cells in culture and in aging skin in vivo. *Proc. Natl. Acad. Sci. U. S. A.* 92, 9363–9367.

(4) Eu, J.P., Liu, L., Zeng, M., Stamler, J.S., 2000. An apoptotic model for nitrosative stress. *Biochemistry* 39, 1040–1047.

(5) Hanada, S., Harada, M., Kumemura, H., Bishr Omary, M., Koga, H., Kawaguchi, T., Taniguchi, E., Yoshida, T., Hisamoto, T., Yanagimoto, C., Maeyama, M., Ueno, T., Sata, M., 2007. Oxidative stress induces the endoplasmic reticulum stress and facilitates inclusion formation in cultured cells. *J. Hepatol.* 47, 93–102.

(6) Hayashi, T., Matsui-Hirai, H., Miyazaki-Akita, A., Fukatsu, A., Funami, J., Ding, Q.F.,

Kamalanathan, S., Hattori, Y., Ignarro, L.J., Iguchi, A., 2006. Endothelial cellular senescence is inhibited by nitric oxide: implications in atherosclerosis associated with menopause and diabetes. *Proc. Natl. Acad. Sci. U. S. A.* 103, 17018–17023.

(7) Hayashida, K., Kume, N., Minami, M., Kita, T., 2002. Lectin-like oxidized LDL receptor-1 (LOX-1) supports adhesion of mononuclear leukocytes and a monocyte-like cell line THP-1 cells under static and flow conditions. *FEBS Lett.* 511, 133–138.

(8) Kimura, T., Nakagawa, K., Kubota, H., Kojima, Y., Goto, Y., Yamagishi, K., Oita, S., Oikawa, S., Miyazawa, T., 2007. Food-grade mulberry powder enriched with 1-deoxynojirimycin suppresses the elevation of postprandial blood glucose in human. *J. Agric. Food Chem.* 55, 5869–5874.

(9) Kume, N., Cybulsky, M.I., Gimbrone Jr., M.A., 1992. Lysophosphatidylcholine, a component of atherogenic lipoproteins, induces mononuclear leukocyte adhesion molecules in cultured human and rabbit arterial endothelial cells. *J. Clin. Invest.* 90, 1138–1144.

(10) Lakatta, E.G., Levy, D., 2003. Arterial and cardiac aging: major shareholders in cardiovascular disease enterprises: Part I: aging arteries: a “set up” for vascular disease. *Circulation* 107, 139–146.

(11) Minamino, T., Komuro, I., 2007. Vascular cell senescence: contribution to atherosclerosis. *Circ. Res.* 100, 15–26.

(12) Minamino, T., Miyauchi, H., Yoshida, T., Ishida, Y., Yoshida, H., Komuro, I., 2002. Endothelial cell senescence in human atherosclerosis: role of telomere in endothelial dysfunction. *Circulation* 105, 1541–1544.

(13) Molina-Jiménez, M.F., Sánchez-Reus, M.I., Andres, D., Cascales, M., Benedi, J., 2004. Neuro-protective effect of fraxetin and myricetin against rotenone-induced apoptosis in neuroblastoma cells. *Brain Res.* 1009, 9–16.

(14) Mudra, M., Ercan-Fang, N., Zhong, L., Furne, J., Levitt, M., 2007. Influence of mulberry leaf extract on the blood glucose and breath hydrogen response to ingestion of 75 g sucrose by type 2 diabetic and control subjects. *Diabetes Care* 30, 1272–1274.

(15) Nakagawa, K., Kubota, H., Kimura, T., Yamashita, S., Tsuzuki, T., Oikawa, S., Miyazawa, T., 2007. Occurrence of orally administered mulberry 1-deoxynojirimycin in rat plasma. *J. Agric. Food Chem.* 55, 8928–8933.

(16) Nakagawa, K., Kubota, H., Tsuzuki, T., Kariya, J., Kimura, T., Oikawa, S., Miyazawa, T., 2008. Validation of an ion trap tandem mass spectrometric analysis of mulberry 1-deoxynojirimycin in human plasma: application to pharmacokinetic study. *Biosci. Biotechnol. Biochem.* 72, 2210–2213.

(17) Piga, R., Naito, Y., Kokura, S., Handa, O., Yoshikawa, T., 2007. Short-term high glucose exposure

induces monocyte-endothelial cells adhesion and transmigration by increasing VCAM-1 and MCP-1 expression in human aortic endothelial cells. *Atherosclerosis* 193, 328–334.

(18) Redmond, E.M., Morrow, D., Kundimi, S., Miller-Graziano, C.L., Cullen, J.P., 2009. Acetaldehyde stimulates monocyte adhesion in a P-selectin- and TNFalpha-dependent manner. *Atherosclerosis* 204, 372–380.

(19) Rogers, S.C., Zhang, X., Azhar, G., Luo, S., Wei, J.Y., 2013. Exposure to high or low glucose levels accelerates the appearance of markers of endothelial cell senescence and induces dysregulation of nitric oxide synthase. *J. Gerontol. A Biol. Sci. Med. Sci.* 68, 1469–1481.

(20) Shinohara, N., Tsuduki, T., Ito, J., Honma, T., Kijima, R., Sugawara, S., Arai, T., Yamasaki, M., Ikezaki, A., Yokoyama, M., Nishiyama, K., Nakagawa, K., Miyazawa, T., Ikeda, I., 2012. Jacaric acid, a linolenic acid isomer with a conjugated triene system, has a strong antitumor effect in vitro and in vivo. *Biochim. Biophys. Acta* 1821, 980–988.

(21) Takahashi, M., Ikeda, U., Masuyama, J., Kitagawa, S., Kasahara, T., Shimpo, M., Kano, S., Shimada, K., 1996. Monocyte-endothelial cell interaction induces expression of adhesion molecules on human umbilical cord endothelial cells. *Cardiovasc. Res.* 32, 422–429.

(22) Tsuduki, T., Nakamura, Y., Honma, T., Nakagawa, K., Kimura, T., Ikeda, I., Miyazawa, T., 2009.

Intake of 1-deoxynojirimycin suppresses lipid accumulation through activation of the beta-oxidation system in rat liver. *J. Agric. Food Chem.* 57, 11024–11029.

(23) Tsuduki, T., Kikuchi, I., Kimura, T., Nakagawa, K., Miyazawa, T., 2013a. Intake of mulberry 1-deoxynojirimycin prevents diet-induced 1 obesity through increases in adiponectin in mice. *Food Chem.* 139, 16–23.

(24) Tsuduki, T., Kuriyama, K., Nakagawa, K., Miyazawa, T., 2013b. Tocotrienol (unsaturated vitamin E) suppresses degranulation of mast cells and reduces allergic dermatitis in mice. *J. Oleo Sci.* 62, 825–834.

(25) Tsuzuki, T., Kawakami, Y., 2008. Tumor angiogenesis suppression by α-eleostearic acid, a linolenic acid isomer with a conjugated triene system, via peroxisome proliferator-activated receptor g. *Carcinogenesis* 29, 797–806.

(26) Tsuzuki, T., Tanaka, K., Kuwahara, S., Miyazawa, T., 2005. Synthesis of the conjugated trienes 5E,7E,9E,14Z,17Z-eicosapentaenoic acid and 5Z,7E,9E,14Z,17Z-eicosapentaenoic acid, and their induction of apoptosis in DLD-1 colorectal adenocarcinoma human cells. *Lipids* 40, 147–154.

(27) Tsuzuki, T., Kambe, T., Shibata, A., Kawakami, Y., Nakagawa, K., Miyazawa, T., 2007. Conjugated EPA activates mutant p53 via lipid peroxidation and induces p53-dependent apoptosis in DLD-1

colorectal adenocarcinoma human cells. *Biochim. Biophys. Acta* 1771, 20–30.

(28) Watson, A.A., Fleet, G.W.J., Asano, N., Molynerux, R.J., Nash, R.J., 2001. Polyhydroxylated alkaloids—natural occurrence and therapeutic applications. *Phytochemistry* 56, 265–295.

(29) Yagi, M., Kouno, T., Aoyagi, Y., Murai, H., 1976. Structure of moranoline, a piperidine alkaloid from Morus species. *Nippon Nogei Kagaku Kaishi* 50, 571–572.

(30) Yanaka, M., Honma, T., Sato, K., Shinohara, N., Ito, J., Tanaka, Y., Tsuduki, T., Ikeda, I., 2011. Increased monocytic adhesion by senescence in human umbilical vein endothelial cells. *Biosci. Biotechnol. Biochem.* 75, 1098–1103.

(31) Yokoi, T., Fukuo, K., Yasuda, O., Hotta, M., Miyazaki, J., Takemura, Y., Kawamoto, H., Ichijo, H., Ogihara, T., 2006. Apoptosis signal-regulating kinase 1 mediates cellular senescence induced by high glucose in endothelial cells. *Diabetes* 55, 1660–1665.

(32) Zhong, W., Zou, G., Gu, J., Zhang, J., 2010. L-arginine attenuates high glucose-accelerated senescence in human umbilical vein endothelial cells. *Diabetes Res. Clin. Pract.* 89, 38–45.

(33) Zou, L., Yang, S., Champattanachai, V., Hu, S., Chaudry, I.H., Marchase, R.B., Chatham, J.C., 2009. Glucosamine improves cardiac function following trauma-hemorrhage by increased protein O-GlcNAcylation and attenuation of NF-kB signaling. *Am. J. Physiol. Heart Circ. Physiol*. 296, H515–

H523.

(34) E S, Kijima R, Honma T, Yamamoto K, Hatakeyama Y, Kitano Y, Kimura T, Nakagawa K, Miyazawa T, Tsuduki T.1-Deoxynojirimycin attenuates high glucose-accelerated senescence in human umbilical vein endothelial cells. Exp Gerontol. 2014 Jul; 55:63-9.

Intake of mulberry 1-deoxynojirimycin prevents colorectal cancer in mice

1. Abstract

The effect of 1-deoxynojirimycin (DNJ), a caloric restriction (CR) mimetic, was examined in ICR mice with AOM (azoxymethane)/DSS (Dextran sodium sulfate)-induced colorectal cancer. AOM is a carcinogen (10mg/kg body weight), and 2%DSS (w/v) used as a colitis-inducing agent. Mice were separated into 5 groups: a group without colorectal cancer fed a normal diet (CO- group), and groups with colorectal cancer fed a normal diet (CO+ group), a calorie-restricted diet (CR group), and diets including 0.02% and 0.1% DNJ (L-DNJ and H-DNJ groups). The tumor incidence and number were reduced significantly in the CR group compared to the CO+ group, and were also suppressed in a dose-dependent manner by 1-deoxynojirimycin. mRNA for anti-apoptotic Bcl-2 was decreased and that for pro-apoptotic Bax was increased in the carcinoma tissue of CR, L-DNJ and H-DNJ groups. These results suggest that CR and 1-deoxynojirimycin inhibit growth of colorectal cancer by inducing apoptosis in an induced cancer model in mice.

2. Abbreviations

DNJ: 1-Deoxynojirimycin

CRC: Colorectal Cancer

CR: Caloric Restriction

AOM: Azoxymethane

DSS: Dextran Sodium Sulfate

Bax: Bcl-2 associated X protein

Bcl-2: B-cell Lymphoma 2

3. Introduction

Cancer is the leading cause of morbidity and mortality worldwide, with approximately 14 million new cases and 8.2 million cancer-related deaths in 2012. [1] More than 60% of new cases annually occur in Africa, Asia and Central and South America, and among these, colorectal cancer is a major cause of tumor-related morbidity and mortality. [1,2] This disease develops due to long-term exposure to environmental factors. [3] In Japan, rapid Westernization of diet has increased the incidence and mortality of colorectal cancer, and this suggests that dietary treatment, especially caloric restriction (CR), may be effective for disease prevention. CR has beneficial effects on cancer prevention, with one study showing that the incidence of neoplasia with CR was significantly lower than that with an *ad libitum* diet. [4,5] However, CR is accompanied by considerable stress in humans, which makes it difficult to use as a method for cancer prevention.

1-Deoxynojirimycin (DNJ) is a D-glucose analogue that is a characteristic constituent of mulberry (Moraceae) leaves. Dietary mulberry DNJ may be beneficial for suppression of abnormally high blood glucose. [6] In addition, we have shown anti-obesity and anti-lipid peroxidation effects of DNJ, with decreased serum insulin and glucose, improved carbohydrate metabolism, and decreased lipid peroxide levels. [7] These beneficial effects may occur because DNJ can reduce the bioavailability of glucose and

have a CR effect. Moreover, DNJ intake showed changes in lipid metabolic parameters like CR. [7] Cancer cells require larger amounts of glucose than normal cells, which suggests that growth of these cells might be inhibited by DNJ. [8,9]

Screening for agents for colorectal cancer prevention has been carried out in mouse models using the potent carcinogen azoxymethane (AOM), which induces colorectal cancers at a high incidence. [10] Dextran sodium sulfate (DSS), a colitis-inducing agent, can be used after AOM to make a two-stage mouse colorectal cancer model. [11,12] In this study, we used this two-stage model to examine the effect of DNJ on colorectal cancer. We also examined the mechanism of the DNJ effect by measuring the levels of apoptosis-related genes.

4. Materials and Methods

4.1. Materials

DNJ was extracted from mulberry leaves (Morus alba) and purified using ion-exchange chromatography followed by recrystallization. [13] The purity of DNJ was shown to be >98% by hydrophilic interaction liquid chromatography with hybrid quadrupole/linear ion trap tandem mass spectrometry (HILIC-QTRAP MS/MS). [7] NaCl, AOM, DSS, miglitol and 10% formalin were purchased from Wako Pure Chemicals Industries (Osaka, Japan).

4.1. Animals and diets

All procedures were performed in accordance with the Animal Experiment Guidelines of Tohoku University. The animal protocol was approved by the Animal Use Committee at Tohoku University. Male ICR mice (n=100, 3 weeks of age) and CE-2 (a control diet) were obtained from Japan Clea (Tokyo, Japan). Mice were housed with ten in each cage and with free access to the respective diets and distilled water in a temperature- and humidity-controlled room with light cycles of 12 h on and 12 h off. [14] After being acclimatized to the control diet for one week, the 100 mice were randomly divided into 5 groups: control diet-fed mice without colorectal cancer inducement (CO-); and control (CO+), calorie-restricted (CR), low DNJ (L-DNJ) and high DNJ (H-DNJ) diet-fed mice with colorectal cancer inducement (n=20 per group).

The experimental protocol is shown in Figure 1. The CO+, CR, L-DNJ and H-DNJ groups received a single intraperitoneal injection of AOM in sterile saline at a dose of 10 mg/kg body weight to induce colorectal cancer. Starting one week after the injection, animals received 2% DSS in drinking water for one week to promote tumor progression. The CO- group received a single intraperitoneal injection of sterile saline only. The CO- and CO+ groups were fed CE-2 diet only. The CR, L-DNJ and H-DNJ groups were fed CE-2 diet for three weeks from the start of the experiment. Then, the CR group was fed every other day with CE-2 diet for 12 weeks, starting 1 week after cessation of DSS exposure. The L-DNJ and H-DNJ groups were fed CE-2 diet containing 0.02% and 0.1% DNJ, respectively, for 13 weeks, starting one week after cessation of DSS exposure. At the end of the 16-week period (21 weeks old), the mice were weighed and blood samples were collected after decapitation. Liver, kidney, pancreas, epididymis adipose tissue, and colon tissue were removed and weighed. The number of colorectal tumors detectable with the naked eye was measured. Serum was isolated by cold centrifugation at 1000×g for 15 min at 4°C (CAX-370 Hybrid Refrigerated Centrifuges, Tomy Digital Biology, Tokyo, Japan). Serum and tissue were stored at −80°C until use.

4.2. Histological analysis of colon tissue

Colon tissue with or without tumors was fixed in 10% formalin and embedded in paraffin. [15] Vertical

sections (5 μm) were cut, mounted on glass slides, stained with hematoxylin and eosin (H&E), and observed using a microscope (BZ-9000; Keyence, Osaka, Japan).

4.4 Biochemical analyses of serum and liver

To confirm a CR effect, biochemical analyses of serum and liver samples were performed as described previously.[7, 16] Triacylglycerol (TG) and total cholesterol (TC) levels in serum and liver, and phospholipid (PL), aspartate aminotransferase (AST), alanine aminotransferase (ALT), and glucose in serum were measured using commercial kits (Wako Pure Chemical, Osaka, Japan). The PL content in liver was determined using the method described by Rouser (1970).[17] Insulin levels in serum were determined using an ELISA kit (Shibayagi, Shibukawa, Japan).

4.5. mRNA expression analyses

For real-time quantitative reverse transcriptase PCR (qRT-PCR), total RNA was isolated from colon (tumor and normal tissues) using a RNeasy Mini Kit (Qiagen, Valencia, CA), after elution with 30 μl of RNase-free water, and stored at −80 °C until use.[18] To quantify expression of genes, the mRNA levels of β-actin, B-cell lymphoma 2 (Bcl-2), Bcl-2 associated X protein (Bax) and sirtuin 1 (Sirt1) were determined using a TP870 Thermal Cycler Dice Real Time System (Takara Bio, Otsu, Japan). This system allows real-time

quantitative detection of PCR products by measuring the increase in fluorescence caused by binding of SYBR green to double-stranded DNA. cDNA was synthesized from the total RNA in colon using a Ready-To-Go T-Primed First-Strand Kit (GE Healthcare, UK). The cDNA was subjected to PCR amplification using SYBR® Premix Ex Taq™ (Perfect Real Time, Takara Bio) and gene-specific primers for β-actin, Bcl-2, BAX or Sirt1. Primer sequences were as follows: β-actin (forward) 5′-AGT GTG ACG TTG ACA TCC GTA-3′, β-actin (reverse) 5′-GCC AGA GCA GTA ATC TCC TTC T - 3′, Bcl-2 (forward) 5′-TGT GGT CCA TCT GAC CCT CC-3′, Bcl-2 (reverse) 5′-ACA TCT CCC TGT TGA CGC TCT-3′, BAX (forward) 5′-TGA AGA CAG GGG CCT TTT TG-3′, BAX (reverse) 5′-AAT TCG CCG GAG ACA CTC G-3′, Sirt1 (forward) 5′-GAC GAT GAC AGA ACG TCA CAC-3′, Sirt1 (reverse) 5′-CGA GGA TCG GTG CCA ATC A-3′. The PCR conditions were 95°C for 10 s, and then 95°C for 5 s and 60°C for 31 s over 40 cycles for each gene. Melting curve analysis was performed following each reaction to confirm the presence of a single reaction product. The cycle threshold (CT) represents the PCR cycle at which the reporter fluorescence increased above a baseline signal. The ratio between the β-actin content in standard and test samples was defined as the normalization factor.

4.6. Determination of lipid peroxides

To examine the reduction of oxidative stress caused by CR, the levels of thiobarbituric acid reactive

substances (TBARS) in serum and liver were determined. [7, 14] To examine oxidative stress caused by AOM and DSS in colon tissue, TBARS level in normal colon tissue was determined. [19]

4.7. DNJ concentration in colorectal cancer and normal tissue

DNJ concentrations in colon tissue (tumor or normal) were determined using HILIC MS/MS. [17] In brief, a 1:10 dilution of colorectal cancer or normal tissue homogenate (500 μL), 100 μL of 0.1 μg/mL miglitol (internal standard) and 600 μl of acetonitrile were mixed by sonicating for 1 min and vortexing for 30 s. After centrifugation at 8,000×g for 10 min at 4°C (CAX-370), the supernatant was collected. A 5-μL aliquot of the resulting extract was subjected to HILIC-MS/MS using a Shimadzu liquid chromatograph and a 4500-tandem mass spectrometer (AB Sciex, Tokyo, Japan). Under positive ion electrospray ionization conditions, MS/MS parameters were optimized with DNJ and miglitol. Samples (5 μL each) were separated on a HILIC column (TSK gel Amide-80, 4.6 mm × 150 mm; Tosoh, Tokyo, Japan), eluted with a mixture of acetonitrile and water (675:325, v/v) containing 6.5 mM ammonium formate (pH 5.5) at a flow rate of 0.2 ml/min and a temperature of 40°C. Post-column, DNJ was detected by HILIC-MS/MS with multiple reaction monitoring for transition of the parent ion to the product ion. DNJ concentrations were calculated using a calibration curve.

4.8. Statistical analysis

Results are expressed as the mean ± standard error of the mean (SE). Data were analyzed using a one-way ANOVA with a Tukey-Kramer test for multiple comparisons among three or four groups. A difference was considered to be significant at $P < 0.05$.

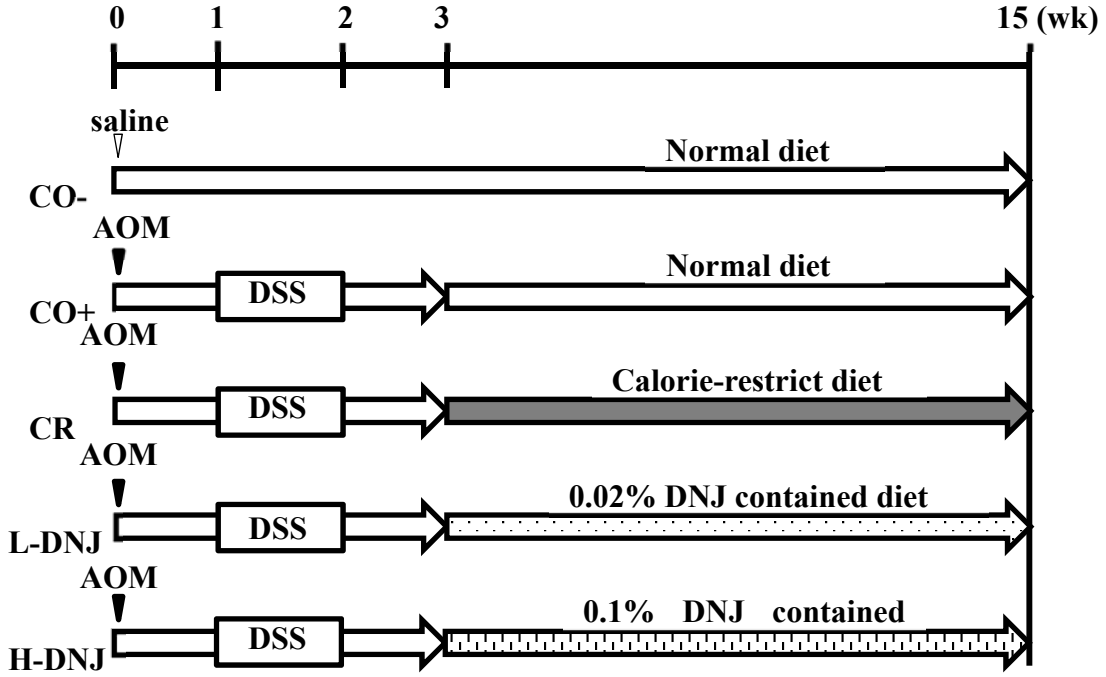

Figure 1. Study design. The CO− group received a single intraperitoneal injection of saline and a normal diet with no more treatment. The CO+, CR, L DNJ and H DNJ groups received a single intraperitoneal injection of AOM and 2% DSS in drinking water for 7 days, starting 1 week after the injection. From the third week, the groups received normal, caloric restricted, 0.02% DNJ and 0.1% DNJ diets, respectively. After 16 weeks, all mice were sacrificed. AOM, azoxymethane; DNJ, 1 deoxynojirimycin; DSS, dextran sulfate sodium.

5. Results

5.1. Effects of caloric restriction and DNJ on growth parameters

There were significant decreases in food and energy intake in the CR group compared to the CO- and CO+ groups. The CR group had caloric restriction of about 20% compared to the CO+ group. In contrast, there were significant increases in food and energy intake in the H-DNJ group compared to the CO- group (Table 1). There were no significant differences in body weight and tissue weights among the groups with induced colorectal cancer.

5.2. Effects of caloric restriction and DNJ on tumor formation

The number of colonic tumors visible with the naked eye was counted after sacrifice (Figure 2-I). H&E staining of colon tissues to confirm the occurrence of a tumor (adenoma and adenocarcinoma) showed colon inflammation (Figure 2-IIB), adenoma (Figure 2-IIC) and adenocarcinoma (Figure 2-IID) in mice with induced cancer, but normal tissue (Figure 2-IIA) in the control group (CO-). Tumor incidences and numbers are shown in Figure 3. Compared to the CO+ group, there was a 28% decrease in tumor incidence in the CR group (Figure 3-I), and 5.2% and 31.5% decreases in the L-DNJ and H-DNJ groups, respectively. There were also significant decreases in the number of tumors in the CR, L-DNJ, and H-DNJ groups compared to the CO+ group (Figure 3-II). The incidence and number decreased in a DNJ dose-dependent

manner, and the results in the H-DNJ group were like those in the CR group.

5.3. Effects of caloric restriction and DNJ on serum and liver parameters

To investigate the effects of caloric restriction and DNJ on lipid and carbohydrate metabolism, serum levels of TG, TC, PL, glucose and insulin were determined (Table 2). There were significant increases in TC and PL in the L-DNJ group compared to the CO+, CR and H-DNJ groups. There was a significant decrease in insulin in the CR, L-DNJ and H-DNJ groups compared to the CO+ group. To evaluate the safety of caloric restriction and DNJ, serum and liver TBARS and serum ALT and AST levels were measured. There were significant decreases in serum and liver TBARS in the CR and H-DNJ groups compared to the CO- and CO+ groups, and TBARS decreased dose-dependently with DNJ. There were significant decreases in serum AST in the CR and H-DNJ group compared to the CO+ group. To investigate the effects of caloric restriction and DNJ on lipid metabolism, liver levels of TG, TC, and PL were determined (Table 2). There were no significant differences in liver parameters among the groups with induced colorectal cancer. There were no significant differences in serum and liver parameters between the CO- and CO+ groups. To investigate the effects of caloric restriction and DNJ on the oxidative stress caused by AOM and DSS in normal colon tissue, TBARS levels in the colon were determined (Table 2). There was significant increase in colon TBARS in the CO+ group compared to the CO- group. There were significant decreases in colon

TBARS in CR, L-DNJ and H-DNJ groups compared to the CO+ group, and TBARS decreased dose-dependently with DNJ.

5.4. Effects of caloric restriction and DNJ on apoptosis

To examine the tumor suppression mechanism, the mRNA levels of two apoptosis-related genes (Bcl-2 and BAX) were measured. There were significant increases in mRNA for pro-apoptotic Bax in the CR and H-DNJ groups compared to the CO+ and L-DNJ groups (Figure 4-I), and significant decreases in mRNA for the anti-apoptotic gene Bal-2 in the CR group compared to the CO+ group, with a tendency for decreases in the L-DNJ and H-DNJ groups (Figure 4-II). The mRNA levels for the two genes varied dose-dependently with DNJ. These findings suggest that caloric restriction and DNJ induce apoptosis of cancer cells. In addition, the caloric restriction-related gene Sirt1 was examined as a caloric restriction marker (Figure 4-III). There were significant increases in mRNA for Sirt1 in the CR group compared to the CO+ group, and tendencies for increases in the L-DNJ and H-DNJ groups.

5.5 DNJ concentration in colorectal cancer and normal tissues

To determine whether DNJ is absorbed in colon tissue, DNJ was measured in normal and tumor colon tissues. DNJ was not found in mice without DNJ intake. The DNJ concentration in the H-DNJ group was

significantly higher than that in the L-DNJ group in normal tissue (0.448 ± 0.114 vs. 0.089 ± 0.013 ng/g) and tumor tissue (1.03 ± 0.09 vs. 0.204 ± 0.048 ng/g). The DNJ concentration in tumor tissue was significantly higher than that in normal tissue.

Table1. Effect of calorie restriction and DNJ on growth parameters in colon cancer-induced male mice.

	CO-	CO+	CR	L-DNJ	H-DNJ
Food intake (g/d)	5.41 ± 0.04 ^{b}	5.69 ± 0.08 ^{bc}	4.45 ± 0.07 ^{a}	5.66 ± 0.09 ^{bc}	5.72 ± 0.08 ^{c}
Energy intake (kcal/day)	18.7 ± 0.15 ^{b}	19.6 ± 0.28 ^{bc}	15.4 ± 0.20 ^{a}	19.5 ± 0.31 ^{bc}	19.7 ± 0.27 ^{c}
Final body weight (g)	44.5 ± 0.91	43.8 ± 0.79	41.4 ± 0.32	43.0 ± 0.39	41.7 ± 0.67
Tissue weight (g/100g body weight)					
Liver	4.09 ± 0.06	4.49 ± 0.13	4.33 ± 0.15	4.47 ± 0.09	4.38 ± 0.13
Pancreas	0.85 ± 0.03	0.93 ± 0.04	0.90 ± 0.04	0.93 ± 0.04	0.92 ± 0.04
Kidney	1.82 ± 0.03 ^{a}	1.92 ± 0.05 ^{ab}	1.90 ± 0.04 ^{ab}	2.03 ± 0.04 ^{b}	1.89 ± 0.06 ^{ab}
Epididymis adipose	1.46 ± 0.18 ^{a}	1.09 ± 0.12 ^{ab}	0.79 ± 0.12 ^{b}	0.80 ± 0.11 ^{b}	0.77 ± 0.13 ^{b}

Values are means ±SE, n = 18-20. Means in a row with different letters are significantly different at $P < 0.05$.

Table2. Effect of calorie restriction and DNJ on plasma, liver and colon parameters in colon cancer-induced male mice.

	CO-	CO+	CR	L-DNJ	H-DNJ
Serum					
Triacylglycerol (mmol/L)	1.51 ± 0.09	1.57 ± 0.09	1.50 ± 0.10	1.72 ± 0.14	1.45 ± 0.11
Total cholesterol (mmol/L)	2.32 ± 0.06 ^{ab}	2.19 ± 0.04 ^{a}	2.11 ± 0.06 ^{a}	2.55 ± 0.08 ^{b}	2.23 ± 0.07 ^{a}
Phospholipid (mmol/L)	2.24 ± 0.04 ^{a}	2.15 ± 0.05 ^{a}	2.14 ± 0.07 ^{a}	2.51 ± 0.09 ^{b}	2.24 ± 0.08 ^{a}
Glucose (mmol/L)	4.57 ± 0.20	5.03 ± 0.26	5.00 ± 0.18	4.69 ± 0.21	5.04 ± 0.28
Insulin (mg/L)	0.24 ± 0.03 ^{ab}	0.26 ± 0.04 ^{a}	0.15 ± 0.03 ^{b}	0.15 ± 0.01 ^{b}	0.15 ± 0.01 ^{b}
HOMA-IR	1.00 ± 0.15	1.20 ± 0.20	0.66 ± 0.06	0.65 ± 0.06	0.66 ± 0.07
TBARS (μmol/L)	5.14 ± 0.21 ^{a}	5.47 ± 0.48 ^{a}	4.17 ± 0.23 ^{b}	4.90 ± 0.29 ^{ab}	4.27 ± 0.25 ^{b}
ALT (UI/L)	9.75 ± 0.42	10.4 ± 0.52	10.0 ± 0.54	9.50 ± 0.92	11.5 ± 0.57
AST (UI/L)	53.0 ± 5.44 ^{a}	61.0 ± 7.89 ^{b}	46.5 ± 5.28 ^{a}	44.7 ± 3.32 ^{a}	43.5 ± 2.41 ^{a}
Liver					
Triacylglycerol (μmol/g)	12.2 ± 1.13	8.82 ± 0.84	11.0 ± 1.21	13.0 ± 1.34	10.7 ± 1.39
Total cholesterol (μmol/g)	7.68 ± 0.65	7.84 ± 0.73	7.02 ± 0.20	6.45 ± 0.50	6.55 ± 0.41
Phospholipid (μmol/g)	34.5 ± 0.8	32.7± 1.4	35.4 ± 1.0	35.5 ± 1.2	34.6 ± 1.4
TBARS (nmol/g)	68.9 ± 5.3^{a}	63.6 ± 3.9^{a}	44.7 ± 2.8^{b}	59.5 ± 3.1^{a}	41.1 ± 3.3^{b}
Colon					
TBARS (nmol/g)	8.6 ± 0.7^{a}	21.2 ± 1.3^{c}	14.9 ± 0.9^{b}	18.8 ± 1.0^{c}	13.7 ± 1.1^{b}

Values are means ± SE, n = 18-20. Means in a row with different letters are significantly different at $P <$ 0.05. HOMA-IR, homeostasis model assessment-insulin resistance; TBARS, thiobarbituric acid reactive substances; ALT, alanine transaminase; AST, aspartate aminotransferase.

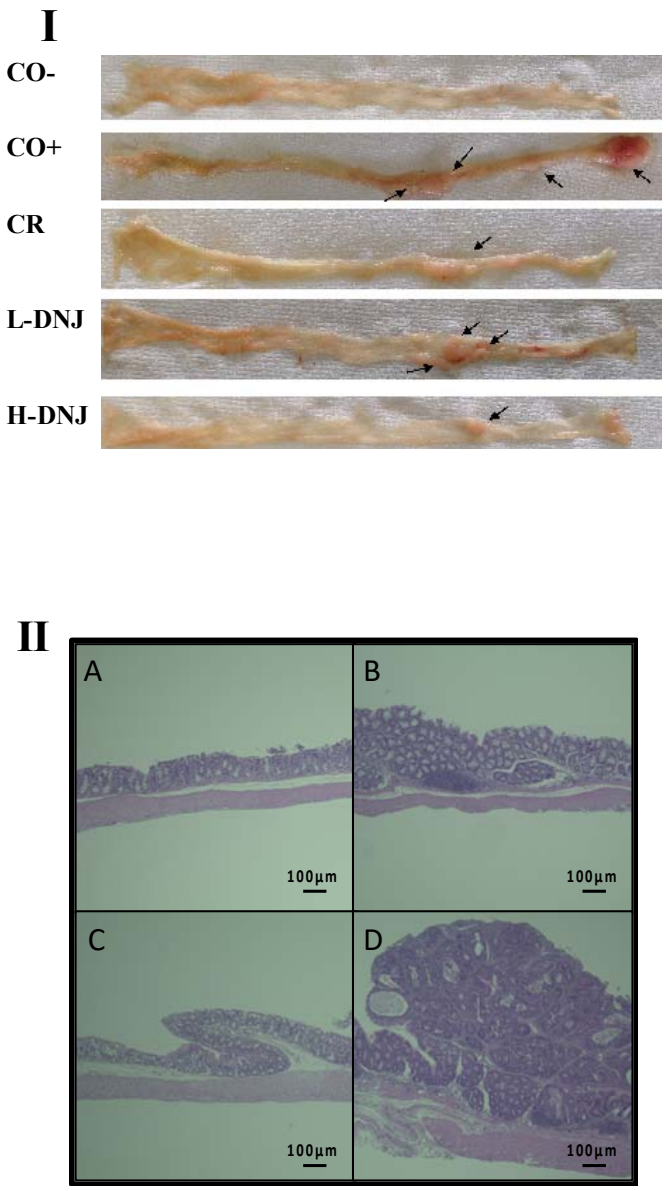

Figure 2 Effect of caloric restriction and DNJ on colon tissue in male mice with induced colorectal cancer. (II) Colon tissue in each group. Arrows indicate tumors. (I) Representative histology images from hematoxylin and eosin stained colon specimens (magnification ×4): (A) normal colon, (B) colon tissue with mild pathology, (C) dysplastic crypts, and (D) well differentiated tubular adenocarcinoma. Bars indicate 100 μm.

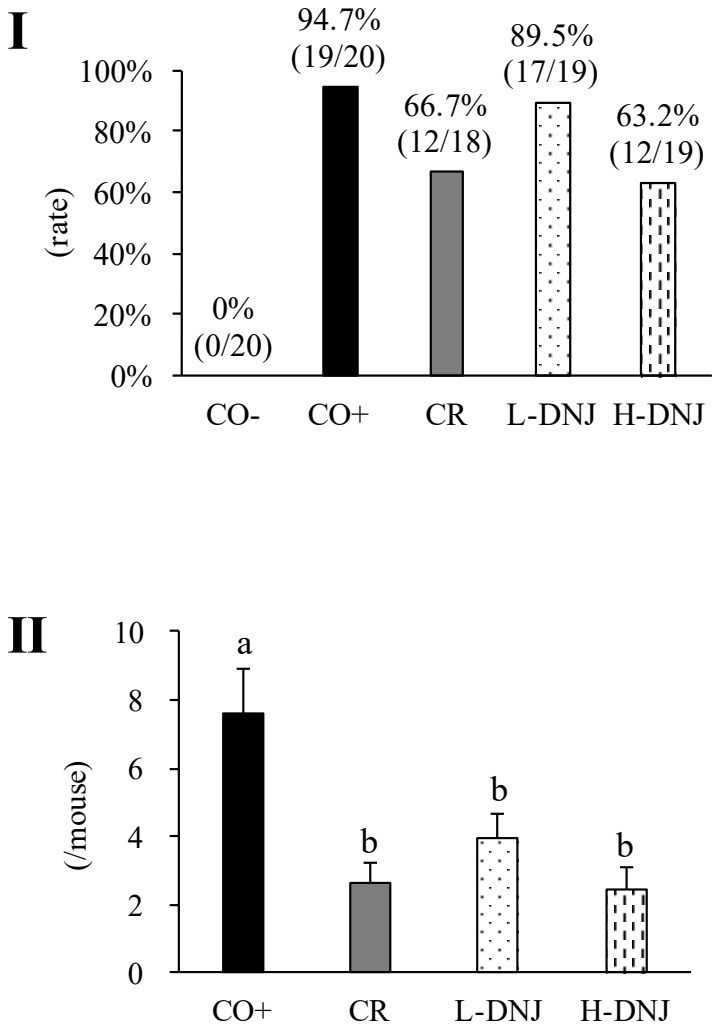

Figure 3 Effect of caloric restriction and DNJ on tumor incidence (I) and number (II) in male mice with induced colorectal cancer. Values are means ± SE, n = 18–20. [a, b] $p<0.05$.

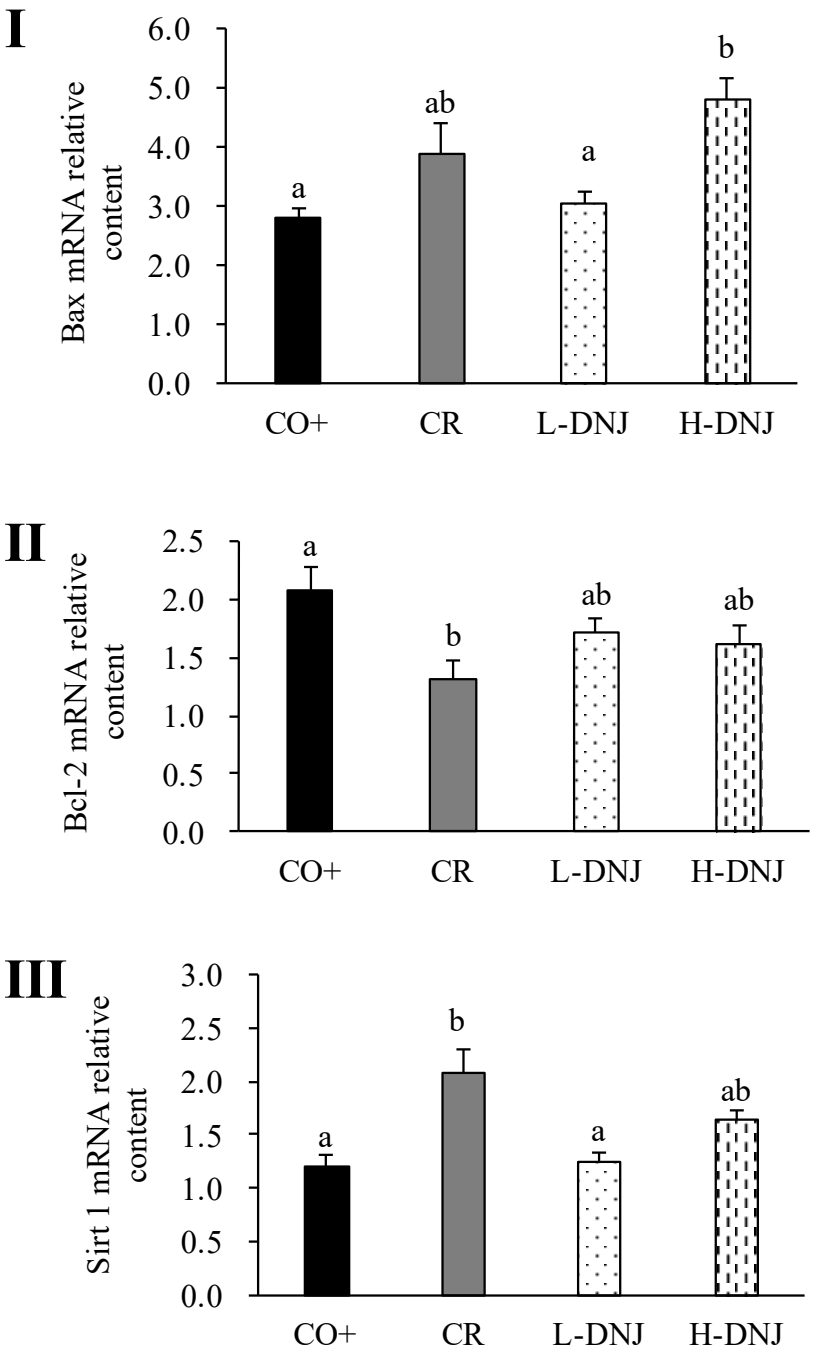

Figure 4 Effect of caloric restriction and DNJ on BAX (I), Bcl 2 (II), and Sirt 1 (III) mRNA levels in male mice with induced colorectal cancer. Values are means ± SE, n = 18–20. [a, b] $p<0.05$.

6. Discussion

In this study, we showed that caloric restriction inhibits AOM/DSS-induced colorectal cancer in ICR mice, and that DNJ suppresses this disease through a caloric restriction-like mechanism. This is the first report of DNJ on colorectal cancer.

Cancer cells require more energy, and especially more glucose, for growth compared to normal cells. This is referred to as the Warburg effect. [8, 20] Therefore, we speculated that caloric restriction can inhibit the growth of tumor cells. In this study, the growth of mice was not particularly affected by caloric restriction, since there was only 20% restriction in the CR group, but colorectal tumors were significantly reduced in the CR group compared to the CO+ group. This suggests that caloric restriction can have an inhibitory effect on colorectal cancer. Similarly, Reddy et al. (1987) reported that 30% caloric restriction reduced the growth of colorectal cancer significantly. Similar results were also found by Olivo-Marston et al. (2014). [4,15] The suppressive effect of DNJ on development of colorectal cancer occurred in a dose-dependent manner, and DNJ had no significant effect on mouse growth.

Sirt1 is involved in acute and chronic energy limitation, such as fasting and diet restriction, and controls metabolism by deactivating many transcriptional regulatory factors and affecting gene expression. [21, 22] Therefore, we used Sirt1 as a marker to judge the effect of caloric restriction on colorectal cancer tissue.

Sirt1 was increased in the CR group, also we found that sirt1was increased in a DNJ dose-dependent manner. In addition, since the serum insulin concentration and insulin restriction marker HOMA-IR trend was lower in DNJ groups, confirmed in the earlier report, it was objectively shown that DNJ has a metabolism regulation effect. [7] Thus, caloric restriction appears to be involved in one of the tumor suppressor mechanisms of DNJ.

Tumor suppression through caloric restriction occurs through induction of apoptosis in cancer cells. [23] To confirm this mechanism, we measured mRNA levels of the anti-apoptotic gene Bcl-2 and pro-apoptotic gene Bax. [24-26] In caloric restriction, mRNA expression for Bax increased and mRNA for Bcl-2 decreased in cancer cells. Similar results were obtained with DNJ intake, it suggests that DNJ induces apoptosis in cancer cells through the Bcl-2/Bax signaling pathway. These findings are also consistent with the role of DNJ as a caloric restriction mimetic.

Absorption of DNJ was verified in normal and tumor colon tissues, it indicates that DNJ can act directly on cancer cells. In addition, the DNJ concentration in colorectal cancer tissue was higher than that in normal colon tissue in both L-DNJ and H-DNJ groups. The similarity of the structure of DNJ to that of glucose may allow DNJ to be taken into cancer cells because these cells have a high demand for glucose compared to normal cells. [8, 20] Thus, DNJ may have greater effects on cancer cells than on normal cells.

As found previously, the levels of TBARS, an oxidative stress indicator, in serums and livers were reduced by DNJ intake. [7] Moreover, in this study, TBARS level in colon was also reduced by DNJ intake. Oxidative stress promotes cancer, and thus DNJ may inhibit cancer growth by reducing oxidative stress. [27, 28] In addition, oxidative stress greatly affects the immune system such as promotion of inflammation. [11, 12] And, the immune system is closely related to the onset of colorectal cancer, like inflammation. [29, 30] Therefore, DNJ may inhibit cancer growth by affecting the immune system through suppressing oxidative stress.

Caloric restriction is a potential approach to prevention of colorectal cancer, but eliminating food intake is also stressful. Therefore, a caloric restriction mimetic such as DNJ would be ideal for cancer prevention. In this study, we showed the efficacy of DNJ for this purpose. Determination of the proper dose of DNJ and understanding of the detailed mechanism of colorectal cancer development suppression effect, will need further studies [31].

7. References

(1) Bernard WS, Christopher PW. (2014). World cancer report 2014. Lyon: IARC, (Chapter 1).

(2) Half E, Arber N. Colon cancer: preventive agents and the present status of chemoprevention. *Expert Opin Pharmacother* 2009; 10: 211-219.

(3) Tanaka T. Colorectal carcinogenesis: review of human and experimental animal studies. *J Carcinog* 2009; 8: 5.

(4) Olivo-Marston SE, Hursting SD, Perkins SN, et al. Effects of calorie restriction and diet-induced obesity on murine colon carcinogenesis, growth and inflammatory factors, and microRNA expression. *PloS one*. 2014; 9: e94765.

(5) Colman RJ, Anderson RM, Johnson SC, et al. Caloric restriction delays disease onset and mortality in rhesus monkeys. *Science* 2009; 325: 201-204.

(6) Kimura T. Development of mulberry leaf extract for suppressing postprandial blood glucose elevation. In: Rigobelo EC, eds. Rijeka: InTech, 2011: 25-36.

(7) Tsuduki T, Kikuchi I, Kimura T, Nakagawa K, Miyazawa T. Intake of mulberry 1-deoxynojirimycin prevents diet-induced obesity through increases in adiponectin in mice. *Food Chem* 2013; 139: 16-23.

(8) Warburg O. On the origin of cancer cells. *Science* 1956; 123: 309-314.

(9) Seyfried TN, Kiebish MA, Marsh J, Shelton LM, Huysentruyt LC, Mukherjee P. Metabolic management of brain cancer. *Biochim Biophys Acta* 2011; 1807: 577-594.

(10) Derry MM, Raina K, Balaiya V, et al. Grape seed extract efficacy against azoxymethane-induced colon tumorigenesis in A/J mice: interlinking miRNA with cytokine signaling and inflammation. *Cancer Prev Res (Phila)* 2013; 6: 625-633.

(11) Yasui Y, Suzuki R, Miyamoto S, et al. A lipophilic statin, pitavastatin, suppresses inflammation associated mouse colon carcinogenesis. *Int J Cancer* 2007; 121: 2331-2339.

(12) Ock CY, Kim EH, Hong H, et al. Prevention of colitis-associated colorectal cancer with 8-hydroxydeoxyguanosine. *Cancer Prev Res (Phila)* 2011; 4: 1507-1521.

(13) Kimura T, Nakagawa K, Kubota H, et al. Food-grade mulberry powder enriched with 1-deoxynojirimycin suppresses the elevation of postprandial blood glucose in humans. *J Agric Food Chem* 2007; 55: 5869-5874.

(14) Honma T, Shinohara N, Ito J, et al. High-fat diet intake accelerates aging, increases expression of Hsd11b1, and promotes lipid accumulation in liver of SAMP10 mouse. *Biogerontology* 2012; 13: 93-103.

(15) Reddy BS, Wang C-X, Maruyama H. Effect of restricted caloric intake on azoxymethane-induced colon tumor incidence in male F344 rats. *Cancer Res* 1987; 47: 1226-1228.

(16) Honma T, Yanaka M, Tsuduki T, Ikeda I. Increased lipid accumulation in liver and white adipose tissue in aging in the SAMP10 mouse. *Biogerontology* 2011; 13: 93-103.

(17) Rouser G, Fleischer S, Yamamoto A. Two-dimensional thin layer chromatographic separation of polar lipids and determination of phospholipids by phosphorus analysis of spots. *Lipids* 1970; 5: 494-496.

(18) Yanaka M, Honma T, Sato K, et al. Increased monocytic adhesion by senescence in human umbilical vein endothelial cells. *Biosci Biotechnol Biochem* 2011; 75: 1098-1103.

(19) Yamamoto K, E S, Hatakeyama Y, Sakamoto Y, Tsuduki T. High-fat diet intake from senescence inhibits the attenuation of cell functions and the degeneration of villi with aging in the small intestine, and inhibits the attenuation of lipid absorption ability in SAMP8 mice. *J Clin Biochem Nutr* 2015; 57: 204-211.

(20) Seyfried TN, Shelton LM. Cancer as a metabolic disease. *Nutr Metab (Lond)* 2010; 7: 7.

(21) Finkel T, Deng CX, Mostoslavsky R. Recent progress in the biology and physiology of sirtuins. *Nature* 2009; 460: 587-591.

(22) Naqvi A, Hoffman TA, DeRicco J, et al. A single-nucleotide variation in a p53-binding site affects nutrient-sensitive human SIRT1 expression. *Hum Mol Genet* 2010; 19: 4123-4133.

(23) Chang HK, Shin MS, Yang HY, et al. Amygdalin induces apoptosis through regulation of Bax and Bcl-2 expressions in human DU145 and LNCaP prostate cancer cells. *Biol Pharm Bull* 2006; 29: 1597-1602.

(24) Giménez-Cassina A, Danial NN. Regulation of mitochondrial nutrient and energy metabolism by BCL-2 family proteins. *Trends Endocrinol Metab* 2015; 26: 165-175.

(25) Wang Y, Yin RF, Teng JS. Wogonoside induces cell cycle arrest and mitochondrial mediated apoptosis by modulation of Bcl-2 and Bax in osteosarcoma cancer cells. *Int J Clin Exp Pathol* 2015; 8: 63-72.

(26) Zeng G, Shen H, Tang G, et al. A polysaccharide from the alkaline extract of Glycyrrhiza inflata induces apoptosis of human oral cancer SCC-25 cells via mitochondrial pathway. *Tumour Biol* 2015; 36: 6781-6788.

(27) Shinohara N, Tsuduki T, Ito J, et al. Jacaric acid, a linolenic acid isomer with a conjugated triene system, has a strong antitumor effect in vitro and in vivo. *Biochim Biophys Acta* 2012; 1821: 980-988.

(28) Tsuzuki T, Tokuyama Y, Igarashi M, Miyazawa T. Tumor growth suppression by α-eleostearic acid, a linolenic acid isomer with a conjugated triene system, via lipid peroxidation. *Carcinogenesis* 2004; 25: 1417-1425.

(29) Shimizu S, Miyamoto S, Fujii G, et al. Suppression of intestinal carcinogenesis in Apc-mutant mice by limonin. *J Clin Biochem Nutr* 2015; 57: 39-43.

(30) Fujimoto K, Fujii G, Sakurai H, Yoshitome H, Mutoh M, Wada M. Intestinal Peyer's patches prevent tumorigenesis in Apc (Min/+) mice. *J Clin Biochem Nutr* 2015; 56: 43-48.

(31) E S**,** Yamamoto K, Sakamoto Y, Mizowaki Y, Iwagaki Y, Kimura T, Nakagawa K, Miyazawa T, Tsuduki T. Intake of mulberry 1-deoxynojirimycin prevents colorectal cancer in mice. J Clin Biochem Nutr. 2017 Jul;61(1):47-52.

Acknowledge

I would like to express my gratitude to many people who supported my life in Tohoku University. Associated professor Tsuyoshi Tsuduki has been my supervisor for 5 years and half, since I came to Tohoku University as a research student. I am grateful for him, he always led my study to the right direction with insightful advises. His help also including give me advices of presentation styles, let me have chances to attend the academic meetings, give me advises

of my career plan. I also want to give my thanks to my lab mates. We did the experiments together, discussed proposal together, had fun together. They let me had a wonderful research time at here, and left me many good memories. I am grateful for my parents who supported me until now form economically and mentally. I would like to acknowledge the Japan Society for the Promotion of Science (JSPS) scholarship program supported me the last year.

Most of all, great thanks to our God through Jesus Christ.